DØnote 5060-CONF

A Search for the Standard Model Higgs boson using the $ZH \to \nu\bar{\nu}b\bar{b}$ channel in $p\bar{p}$ Collisions at $\sqrt{s} = 1.96$ TeV

The DØ Collaboration
URL: http://www-d0.fnal.gov
(Dated: March 20, 2006)

This note describes a search for the standard model Higgs boson produced in association with the Z boson at DØ, based on an integrated luminosity of 261 pb^{-1} of data. We study the $p\bar{p} \to ZH \to \nu\bar{\nu}b\bar{b}$ channel, which is one of the most sensitive ways to search for light Higgs bosons because of the large $Z \to \nu\bar{\nu}$ and $H \to b\bar{b}$ branching ratios. The analysis starts with a sample of multijet events with large imbalance in transverse momentum. We then select events with two b-tagged jets and search for a peak in their invariant mass distribution. After subtracting the backgrounds, we measure the 95 % C.L. upper limits on the $\sigma(p\bar{p} \to ZH) \times Br(H \to b\bar{b})$ for Higgs masses between 105 and 135 GeV to be 2.5−3.4 pb.

Preliminary Results for Winter 2006 Conferences

I. INTRODUCTION

The Higgs boson is the only particle in the standard model that has not been directly observed. Since the Higgs boson plays a crucial role in the mechanism of electroweak symmetry breaking, it is important to search for it at the Tevatron. LEP experiments provide lower limits on its mass, and electroweak global fits favor a relatively light Higgs boson. Tevatron Run II experiments have the capability to observe a Higgs boson of low mass. Thus, a search for the Higgs boson is one of the most important goals of the DØ and CDF experiments [1],[2].

The $p\bar{p} \to ZH \to \nu\bar{\nu}b\bar{b}$ channel is one of the most sensitive ways to search for a light Higgs boson because of the large $Z \to \nu\bar{\nu}$ and $H \to b\bar{b}$ branching ratios. The product of the cross section and branching fraction is expected to be about 0.01 pb for a light Higgs boson, which is almost as large as that of $WH \to l\nu b\bar{b}$ [3].

The final state has two b jets from Higgs boson decay, and missing transverse energy ($\not\!\!E_T$) due to the two neutrinos from Z decay. The two b jets are boosted along the Higgs momentum direction. Therefore, they tend to be acoplanar in contrast to typical back-to-back QCD dijet production. There are two main sources of the background to this channel. The physics backgrounds are Z+jets, W+jets, electroweak diboson production like WZ and ZZ production, and top quark production with escaping leptons or jets. On the other hand, the instrumental background is caused by multijet events with mismeasurement of the jet energy or misidentification of jets. Selecting events with large $\not\!\!E_T$and two b-tagged jets rejects a large fraction of multijet background. Since trigger and selection criteria rely on jets, good understanding of the calorimeter response and b-tagging are the main ingredients of this analysis.

The preliminary result was reported in Winter 2005 [4]. The purpose of this note is to describe the updated analysis and to be used as input to the combined DØ Higgs boson production limits, where information from the following channels is used [5]: $p\bar{p} \to ZH \to \nu\bar{\nu}b\bar{b}$, $p\bar{p} \to WH \to e\bar{\nu}b\bar{b}$, $p\bar{p} \to WH \to \mu\bar{\nu}b\bar{b}$, $p\bar{p} \to WH \to WWW \to l^{\pm}\nu l^{\pm}\nu X$, and $p\bar{p} \to H \to WW \to l^{\pm}\nu l^{\mp}\bar{\nu}$.

II. DATA SAMPLE AND EVENT SELECTION

The DØ detector [6] has a magnetic central-tracking system surrounded by a uranium/liquid-argon calorimeter, which is contained within a muon spectrometer. The central-tracking system consists of a silicon microstrip tracker (SMT) and a central fiber tracker (CFT), both located within a 2 T superconducting solenoidal magnet. The SMT and CFT have designs optimized for tracking and vertexing capabilities for pseudorapidities $|\eta| < 3$ and 2.5, respectively. The calorimeter has a central section (CC) covering up to $|\eta| \approx 1.1$, and two end calorimeters (EC) extending coverage to $|\eta| \approx 4.2$, all housed in separate cryostats [7]. For particle identification, the calorimeter is divided into an electromagnetic (EM) part followed by fine (FH) and coarse (CH) hadronic sections. Scintillators between the CC and EC cryostats provide additional sampling of developing showers for $1.1 < |\eta| < 1.4$. The muon system resides beyond the calorimeter, and consists of a layer of tracking detectors and scintillation trigger counters in front of 1.8 T toroids, followed by two similar layers behind the toroids which provide muon tracking for $|\eta| < 2$. The luminosity is measured using scintillator arrays located in front of the EC cryostats, covering $2.7 < |\eta| < 4.4$.

A dedicated trigger has been designed to select events with acoplanar jets accompanied by $\not\!\!E_T$ from March 2003 to June 2004. The integrated luminosity is 261 pb^{-1} after the requirement of detector quality. The event selection requires two or three jets with p_T >20 GeV in $|\eta|$ <2.5. Jets are required to pass quality cuts to reject noise and electromagnetic objects and their energies are corrected back to the particle level for detector and physics effects using the standard jet energy scale factors. The correction depends on the p_T and η of jets and is typically 30% for the data and 20% for the simulation. The jet resolution is measured by energy balance of the jet+γ process and is typically $10 - 15\%$ for data and $6 - 10\%$ for the simulation. The difference between the data and simulation is taken into account by smearing the jets in simulation.

The requirements of $\not\!\!E_T > 50$ GeV, azimuthal angle ϕ between two leading jets $< 165°$, and no isolated tracks in the event reject QCD multijet especially back-to-back event topology, $W(\to e\nu, \mu\nu)$+jet, and $Z(\to ee, \mu\mu)$+jet events. H_T, the scalar sum of the jet p_T, is required to be less than 240 GeV for the rejection of $t\bar{t}$ background. To further reduce the background, we define the following variables:

- min$\Delta\phi$ ($\not\!\!E_T$, jets) :
  the minimum of the difference in azimuthal angle ϕ between the direction of $\not\!\!E_T$ and any of the jets,
- $\not\!\!H_T \equiv |\sum_i^{njet} \vec{p_T}|$:
  the magnitude of the opposite vector sum of accepted jet p_T,
- $P_T^{trk} \equiv |-\sum_i^{ntrk} \vec{p_T}|$:
  the magnitude of the opposite vector sum of all tracks' p_T,

- $\Delta\phi(\not\!\!E_T\ ,\ P_T^{trk})$:
  the difference in azimuthal angle ϕ between the direction of $\not\!\!E_T$ and P_T^{trk},
- $\mathrm{A}(\not\!\!E_T\ ,\ \not\!\!H_T\ ) \equiv (\not\!\!E_T\ -\ \not\!\!H_T\ )/(\not\!\!E_T\ +\ \not\!\!H_T\ )$:
  the asymmetry between $\not\!\!E_T$ and $\not\!\!H_T$.

The instrumental background is significantly reduced by requiring: $\not\!\!E_T$ /GeV $> -40 \times \min\Delta\phi(\not\!\!E_T\ ,\ \mathrm{jet}) + 80$, P_T^{trk} > 20 GeV, $\Delta\phi(\not\!\!E_T\ ,\ P_T^{trk}) < 90^\circ$ and $-0.1 < \mathrm{A}(\not\!\!E_T\ ,\ \not\!\!H_T\ ) < 0.2$. The variables listed above are studied in W+jets samples to assure they are well modeled. The comparisons of $\mathrm{A}(\not\!\!E_T\ ,\ \not\!\!H_T\ )$ and $\Delta\phi(\not\!\!E_T\ ,\ P_T^{trk})$ in W+jets data with simulation are shown in FIG.1. FIG.2 shows the scatter plots of $\mathrm{A}(\not\!\!E_T\ ,\ \not\!\!H_T\ )$ and $\Delta\phi(\not\!\!E_T\ ,\ P_T^{trk})$ for data, signal simulation, physics background simulation, and instrumental simulation. The signal and physics simulations have a clear peak around $\mathrm{A}(\not\!\!E_T\ ,\ \not\!\!H_T\ ) \sim 0$ and $\Delta\phi(\not\!\!E_T\ ,\ P_T^{trk}) \sim 0$, which is not the case for the instrumental background simulation. The instrumental background is estimated from the data, which is described in the Section IV. Not all processes that can give rise to instrumental background have been modeled. Nevertheless, the distribution shown in FIG. 2 gives a qualitative understanding of the distribution of this background.

It is difficult to distinguish a b-jet from a light quark jet if it does not satisfy minimal requirements. Jets are called taggable is they fulfill the following requirements. Each jet is required to be matched, within a cone of $\Delta R < 0.5$, to a track-jet with ≥ 2 tracks. Track-jets begin with a seed-track of $p_T > 1$ GeV, to which lower p_T tracks are added if they pass quality cuts and are within $\Delta R < 0.5$ of the current track-jet direction and Δz <2.0 of the current track-jet z position. The track-jet direction and z position is updated upon the addition of each track. The track quality cuts require p_T >1.0 GeV, ≥ 1 SMT hit, and the distance of closest approach to the primary vertex in the transverse and z directions to be less than 2 and 4 mm, respectively. The fraction of taggable jets is measured by the $W(\rightarrow \mu\nu)$+jets data to be 86% per jet. This fraction is a function of the $|\eta|$, p_T, and z coordinates of the primary vertex and is then applied to the simulated jets.

III. SIMULATED EVENT SAMPLE

The following processes are simulated to estimate the signal acceptance and the total number of expected background events:

- $ZH \rightarrow \nu\bar{\nu}b\bar{b}$ production generated by `PYTHIA` [8],
- $t\bar{t}$ production generated by `PYTHIA`,
- The single top (tb and tqb channels) generated by `COMPHEP` [9],
- $WZ \rightarrow l\nu jj$ and $ZZ \rightarrow \nu\bar{\nu}b\bar{b}$ and $\nu\bar{\nu}c\bar{c}$ production with `ALPGEN` [10],
- W+jets events generated with `ALPGEN` including Wj, Wjj, Wcc, and Wcj process, where W decays to $e\nu$, $\mu\nu$, and $\tau\nu$,
- Z+jets events generated with `ALPGEN` including Zj, Zjj, Zcc, and Zcj process, where Z decays to $\nu\bar{\nu}$, ee, $\mu\mu$, and $\tau\tau$,
- Wbb events generated by `ALPGEN` with W decays to $e\nu$, $\mu\nu$, and $\tau\nu$,
- Zbb events generated by `ALPGEN` with Z decays to $\nu\bar{\nu}$, ee, $\mu\mu$, and $\tau\tau$.

The samples generated by `COMPHEP` and `ALPGEN` are passed through `PYTHIA` for showering and hadronization. The next-to-leading order cross section calculations given by `MCFM` are used [11],[12]. The branching ratios of W and Z decays are taken from PDG 2004 [13]. The instrumental background is measured in data, but is also simulated by `PYTHIA` in order to study variables used in the background estimation.

All the samples were processed through the DØ detector simulation (DØgstar [14], based on `GEANT`), the electronics simulation (DØsim), and the reconstruction software (DØreco). Trigger efficiencies, measured in data, were then applied to the simulated events.

IV. INSTRUMENTAL BACKGROUND ESTIMATION

The instrumental background is estimated from the data in the sideband region. The sideband region is defined as $\Delta\phi(\not\!\!E_T\ ,\vec{P}_T^{trk}) > 90°$, instead of $\Delta\phi(\not\!\!E_T\ ,\vec{P}_T^{trk}) < 90°$. The physics backgrounds passing through the final selection tend to be distributed around $\Delta\phi(\not\!\!E_T\ ,\vec{P}_T^{trk}) \sim 0°$, while the instrumental background can be distributed sideband region as well as signal region due to mis-measurement of the jet energy and/or mis-measurement of charged tracks. FIG. 3 shows the $A(\not\!\!E_T\ ,\not\!\!H_T\ )$ for the data in the sideband region and in the signal region data. The number of physics backgrounds after all selection except for the b-tagging is estimated with the Monte Carlo and parameterized by a triple Gaussian function. The remaining contribution is considered as the instrumental background. The instrumental background can be modeled by a polynomial function from the data in the sideband region. Therefore, the data in the signal region can be modeled by a triple Gaussian for physics background plus a polynomial for the instrumental background. The fit, as shown in FIG. 3, predicts the number of instrumental backgrounds before b-tagging to be 696.1±91.4 events, while the number of physics backgrounds are estimated to be 2514.9 events by Monte Carlo. The physics background in the sideband, estimated by simulation, is subtracted from data in the sideband. The level of the correction is ≈ 15%. The corrected data in the sideband is normalized to the expected number of instrumental background events from the fit, and are used for the estimation of the event yields after the b-tagging. FIG.4 shows the p_T of the first and second leading jets, $\not\!\!E_T$, and the invariant mass formed with the two leading jets. The simulation agrees well with data, after accounting for the estimated instrumental background.

V. b-TAG RESULTS

The b-tagging algorithm uses a lifetime probability that is estimated from the tracks associated with a given jet. A small probability corresponds to jets having tracks with large impact parameters that characterize b-hadron decay. We define two samples: One requires the two leading jets to pass the b-tagging condition (double b-tagged sample), the other requires at least one jets to pass the b-tagging condition, where events in the double b-tagged sample are excluded (exclusive single b-tagged sample). The cut value on the lifetime probability is defined by a selection optimization. We cut on a lifetime probability smaller than 1% for the leading jet and 4% for the second leading jets for the double b-tagged sample, and smaller than 0.1% for the exclusive single b-tagged sample. For the simulated jets, we apply b-tag efficiency and charm , τ, and light quark jets tag rate functions, depending on the flavor of the jets. The type of the jets are determined by the simulated hadrons within $\Delta R < 0.5$ of the jet axis. For the instrumental background, we estimate the tag rate from the data in the sideband region. The difference between the tag rate in the sideband and signal regions are taken into account by an extrapolation of the tag rate from sideband to signal region.

TABLE I lists the number of Higgs, background, and observed events for each b-tag requirement. After the double b-tag requirement, 25 events remain, while 27.0 events are expected. The dominant background is vector boson(W or Z) + jets. After the exclusive single b-tag requirement, 106 events remain, while 94.5 events are expected. FIG.5 shows the p_T of the first and second leading jets, $\not\!\!E_T$, and the invariant mass formed with the two leading jets in the exclusive single b-tagged sample. FIG.6 shows the p_T of the first and second leading jets, $\not\!\!E_T$, and the invariant mass formed with the two leading jets in the double b-tagged sample.

VI. CROSS SECTION LIMITS

We search for an excess of events in a dijet mass (M_{jj}) window. The relative resolution of dijet mass is estimated to be ≈ 17% by signal simulation for 105 GeV to 135 GeV of Higgs masses. We define the mass window as the region of $\pm 1.5\sigma$ around the mean determined from the the simulated dijet mass distribution of the signal. No excess over the standard model background is found in the data. We estimate the systematic uncertainty due to trigger efficiency, jet reconstruction efficiency, jet energy scale factor, jet resolution, b-tagging (including taggability), instrumental background estimation, and background cross section. The estimation is performed by varying each source of uncertainty by ± 1 σ and repeating the analysis. TABLE II lists the systematics for each uncertainty and for the double b-tagged sample and exclusive single b-tagged sample. The uncertainty from the integrated luminosity is estimated to be 6.5%.

Eleven double b-tagged events (Thirty three exclusive single b-tagged events) are observed in the dijet mass window of a 115 GeV Higgs. The expected background for the double b-tagged sample (exclusive single b-tagged sample) is 9.4±1.8 (34.0±6.1) events and the expected acceptance of ZH signal for the double b-tagged sample (exclusive single b-tagged sample) is (1.04±0.20)% ((0.99±0.14)%). Same analysis is performed for three other Higgs boson mass points which are 105, 125, and 135 GeV, as summarized in TABLE III and TABLE IV.

TABLE I: Number of expected signal and background events, and observed events in data before b-tag, after single b-tag, and double b-tag. For the ZH and WH channel, the number of candidates is estimated by the simulation with 115 GeV Higgs mass. The inclusive 1 b-tagged sample requires at least one jet to pass a lifetime probability smaller than 4%, the 2 b-tagged sample requires a lifetime probability smaller than 1% for the leading jet and 4% for the second leading jets, and the exclusive 1 b-tagged sample requires at least one jet to pass a lifetime probability smaller than 0.1%, where events in the double b-tagged sample are excluded

	Z+2 or 3 jets	Z+2 or 3 jets inclusive 1 b-tag	Z+2 or3 jets 2 b-tags	Z+2 or 3 jets exclusive 1 b-tag
ZH	0.71	0.62	0.24	0.26
WH	0.54	0.47	0.18	0.20
Zjj	843.3	93.3	1.4	7.9
Zbb	13.1	11.3	4.1	4.7
Wjj	1596.4	260.1	4.2	36.1
Wbb	12.4	10.5	3.6	4.4
$t\bar{t}/tb/tqb$	42.3	33.6	9.0	15.3
WZ/ZZ	7.3	3.4	0.85	1.1
Instrumental background	696.1	142.6	3.9	25.0
Total expectation	3211.0	554.5	27.0	94.5
Observed events	3210	592	25	106

TABLE II: The systematic uncertainties and their sources for $M_H = 115$ GeV. The systematic uncertainties for the other Higgs masses are same level. In addition to these errors, the uncertainty of the integrated luminosity is 6.5%.

	double b-tag		exclusive single b-tag	
Source	Signal Acceptance (%)	Background (%)	Signal Acceptance (%)	Background (%)
Trigger efficiency	6	6	6	6
Jet identification	7	6	7	6
Jet energy scale	7	8	9	11
Jet resolution	5	2	5	2
Taggability	1	1	1	1
b-tag	14	12	3	5
b-tag for instrumental background	-	9	-	8
Instrumental background expectation	-	2	-	3
Background cross section	-	5	-	5
Total	19	19	14	18

If a lepton from a W decay escapes from the detector measurements, the WH signal can be remained in the $\not\!\!E_T$+jets samples, which is not small compared to the estimated ZH signals. Therefore we expect an improvement of the WH sensitivity from this analysis. For the double b-tagged sample, The expected acceptance of WH signal in the dijet mass window of a 115 GeV Higgs for the double b-tagged sample (exclusive single b-tagged sample) is (0.43±0.08)% ((0.42±0.06)%). Four different Higgs boson mass points are summarized in TABLE III and TABLE IV.

The double b-tagged and exclusive single b-tagged analysis are then combined: the limits are derived from the two invariant dijet mass distributions, using a modified frequentist approach, the CL_S method [15] [16]. In this case, the binned distributions are summed over the log-likelihood ratio test statistic. Systematic uncertainties are incorporated into the signal and background expectations using Gaussian sampling of individual uncertainties. Correlations between uncertainties are handled by varying simultaneously for all channels the fluctuations of identical sources. Limits are determined by scaling the signal expectations until the probability for the background-only hypothesis falls below 5% (95% CL). This translates into a cross section limit for $\sigma(p\bar{p} \to ZH) \times B(H \to b\bar{b})$ of 3.2 pb and for $\sigma(p\bar{p} \to WH) \times B(H \to b\bar{b})$ of 7.5 pb at 95% C.L. limit for a Higgs boson mass of 115 GeV. The limits for four Higgs mass points (105, 115, 125, and 135 GeV) are summarized in TABLE V. As shown in FIG. 7, we set 95% C.L. upper limits between 2.5 to 3.4 pb on the cross section for ZH production multiplied by the branching ratio for $H \to b\bar{b}$.

VII. SUMMARY

We have performed a search for ZH associated production in the $\nu\bar{\nu}b\bar{b}$ channel using 261 pb^{-1} of data. We have studied the dijet mass spectrum of the two leading b-tagged jets for Higgs boson masses between 105 and 135 GeV. In the absence of signal, we have set 95% C.L. upper limits between 2.5 to 3.4 pb on the cross section for ZH production

TABLE III: Signal acceptance (including $B(Z \to \nu\bar{\nu})$ =20% or $B(W \to \nu\bar{\nu})$ 10%), number of expected background events, and limits on the the cross section for $\sigma(p\bar{p} \to ZH) \times B(H \to b\bar{b})$ and $\sigma(p\bar{p} \to WH) \times B(H \to b\bar{b})$ at 95% C.L., for M_H = 105, 115, 125, and 135 GeV and for the double b-tagged sample.

Higgs Mass	105 GeV	115 GeV	125 GeV	135 GeV
Data	10	11	10	9
ZH	0.25	0.21	0.15	0.091
(ZH ($H \to b\bar{b}$) channel Acceptance (%))	(0.86 ± 0.16)	(1.04 ± 0.20)	(1.18 ± 0.22)	(1.34 ± 0.24)
WH	0.18	0.15	0.098	0.062
(WH ($H \to b\bar{b}$) channel Acceptance (%))	(0.36 ± 0.07)	(0.43 ± 0.08)	(0.47 ± 0.09)	(0.55 ± 0.10)
Zjj	0.47	0.50	0.39	0.40
Zbb	1.4	1.4	1.4	1.4
Wjj	1.6	1.5	1.6	1.6
Wbb	1.2	1.1	1.2	1.2
$tt/tb/tqb$	2.5	3.0	3.5	4.2
WZ/ZZ	0.67	0.60	0.48	0.36
Instrumental	1.2	1.3	1.2	1.4
TOTAL backgrounds	8.9 ± 1.7	9.4 ± 1.8	9.8 ± 1.8	10.5± 2.0

TABLE IV: Signal acceptance (including $B(Z \to \nu\bar{\nu})$ =20% or $B(W \to \nu\bar{\nu})$ 10%), number of expected background events, and limits on the the cross section for $\sigma(p\bar{p} \to ZH) \times B(H \to b\bar{b})$ and $\sigma(p\bar{p} \to WH) \times B(H \to b\bar{b})$ at 95% C.L., for M_H = 105, 115, 125, and 135 GeV and for the exclusive single b-tagged sample.

Higgs Mass	105 GeV	115 GeV	125 GeV	135 GeV
Data	29	33	37	44
ZH	0.24	0.20	0.14	0.087
(ZH ($H \to b\bar{b}$) channel Acceptance (%))	(0.84 ± 0.11)	(0.99 ± 0.14)	(1.13 ± 0.15)	(1.28 ± 0.15)
WH	0.18	0.14	0.096	0.061
(WH ($H \to b\bar{b}$) channel Acceptance (%))	(0.35 ± 0.05)	(0.42 ± 0.06)	(0.45 ± 0.06)	(0.54 ± 0.06)
Zjj	2.7	2.6	2.4	2.6
Zbb	1.6	1.6	1.6	1.6
Wjj	13.2	13.6	14.1	14.2
Wbb	1.4	1.4	1.5	1.5
$tt/tb/tqb$	4.6	5.6	6.6	7.7
WZ/ZZ	0.78	0.71	0.59	0.48
Instrumental	7.9	8.4	8.3	9.2
TOTAL backgrounds	32.2 ± 5.9	34.0 ± 6.1	35.2 ± 6.0	37.3± 6.6

multiplied by the branching ratio for $H \to b\bar{b}$, using the CL_S method. We added new limits for the exclusive single b-tagged sample and WH associated production in the $\nu\bar{\nu}b\bar{b}$ channel with escape of the lepton to be between 6.3 to 8.3 pb. These results are used for the DØ combined Higgs boson searches [5].

Acknowledgments

We thank the staffs at Fermilab and collaborating institutions, and acknowledge support from the Department of Energy and National Science Foundation (USA), Commissariat à L'Energie Atomique and CNRS/Institut National de Physique Nucléaire et de Physique des Particules (France), Ministry for Science and Technology and Ministry for

TABLE V: Expected and observed 95% C.L. limits for the combined (double b-tagged and exclusive single b-tagged analysis) $ZH \to \nu\bar{\nu}b\bar{b}$ and $WH \to l^{\pm}\nu b\bar{b}$ final state in fully simulated Higgs mass points.

Channel	105 GeV	115 GeV	125 GeV	135 GeV
ZH Combined Expected (pb)	3.1	2.7	2.4	2.1
ZH Combined Observed (pb)	3.4	3.2	2.9	2.5
WH Combined Expected (pb)	7.6	6.3	6.0	5.0
WH Combined Observed (pb)	8.3	7.5	7.4	6.3

Atomic Energy (Russia), CAPES, CNPq and FAPERJ (Brazil), Departments of Atomic Energy and Science and Education (India), Colciencias (Colombia), CONACyT (Mexico), Ministry of Education and KOSEF (Korea), CONICET and UBACyT (Argentina), The Foundation for Fundamental Research on Matter (The Netherlands), PPARC (United Kingdom), Ministry of Education (Czech Republic), Natural Sciences and Engineering Research Council and WestGrid Project (Canada), BMBF (Germany), A.P. Sloan Foundation, Civilian Research and Development Foundation, Research Corporation, Texas Advanced Research Program, and the Alexander von Humboldt Foundation.

---

[1] "Report of the Tevatron Higgs Working Group," hep-ph/0010338.
[2] "Results of the Tevatron Higgs Sensitivity Study," FERMILAB-PUB-03/320-E.
[3] M. L. Ciccolini, S. Dittmaier, M. Krame, Phys. Rev. D68 (2003) 073003.
[4] DØ Collaboration, "A Search for SM Higgs boson using the $ZH \to \nu\bar{\nu}b\bar{b}$ channel in $p\bar{p}$ Collisions at $\sqrt{s} = 1.96$ TeV," DØ note 4774-Conf, http://www-d0.fnal.gov/Run2Physics/WWW/results/higgs.htm.
[5] DØ Collaboration, "Limits on Standard Model Higgs Boson Production," DØ note 5056-Conf, http://www-d0.fnal.gov/Run2Physics/WWW/results/higgs.htm.
[6] DØ Collaboration, "The Upgraded DØ Detector," accepted to Nucl. Instr. and Methods, hep-physics/0507191, Fermilab-Pub-05/341-E.
[7] S. Abachi, *et al.*, "The DØ Detector," Nucl. Instrum. Methods Phys. Res. A **338**, 185 (1994).
[8] T. Sjostrand, P. Eden, C. Friberg, L. Lonnblad, G. Miu, S. Mrenna and E. Norrbin, "High-energy-physics event generation with `PYTHIA`," Comput. Phys. Commun. **135**, (2001) 238.
[9] A. Pukhov *et al.*, `COMPHEP`, hep-ph/9908288 (1999).
[10] M. Mangano *et al.*, "ALPGEN, a generator for hard multiparton processes in hadron collisions," JHEP 0307 001 2003, hep-ph/0206293.
[11] John Campbell and R.K. Ellis, Phys. Rev. D65:113007 (2002), hep-ph/0202176.
[12] John Campbell and R.K. Ellis, "MCFM - Monte Carlo for FeMtobarn processes," http://mcfm.fnal.gov/.
[13] S. Eidelman et al., Phys. Lett. B592, 1 (2004).
[14] Y. Fisyak and J. Womersley, DØ-Note 3191.
[15] W. Fisher, DØ-Note 4975.
[16] T. Junk, Nucl. Instrum. Meth. A434, p.435-443, 1999.
[17] CDF Collaboration, "Search for the Standard Model Higgs boson in the $ZH \to \nu\bar{\nu}b\bar{b}$ channel in $p\bar{p}$ Collisions at $sqrts$=1.96 TeV," CDF-Note 7983.

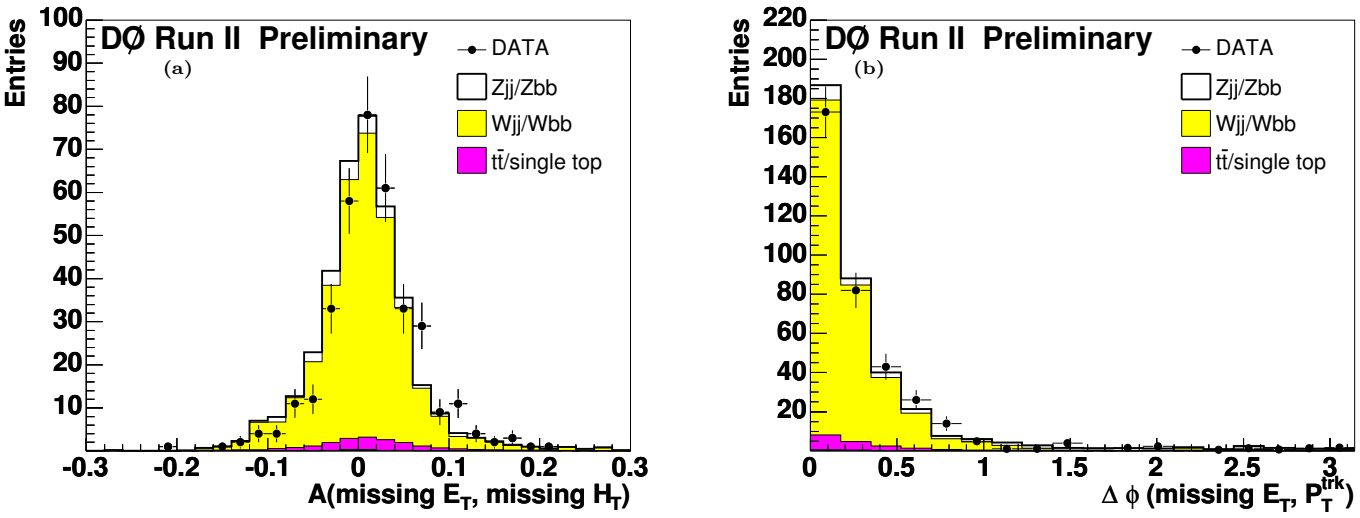

FIG. 1: Distribution of (a): A($\not\!\!E_T$, $\not\!\!H_T$) and (b) : $\Delta\phi(\not\!\!E_T, \vec{P}_T^{trk})$ for the $W+$ jets sample. For both distributions, the simulation agrees well with data.

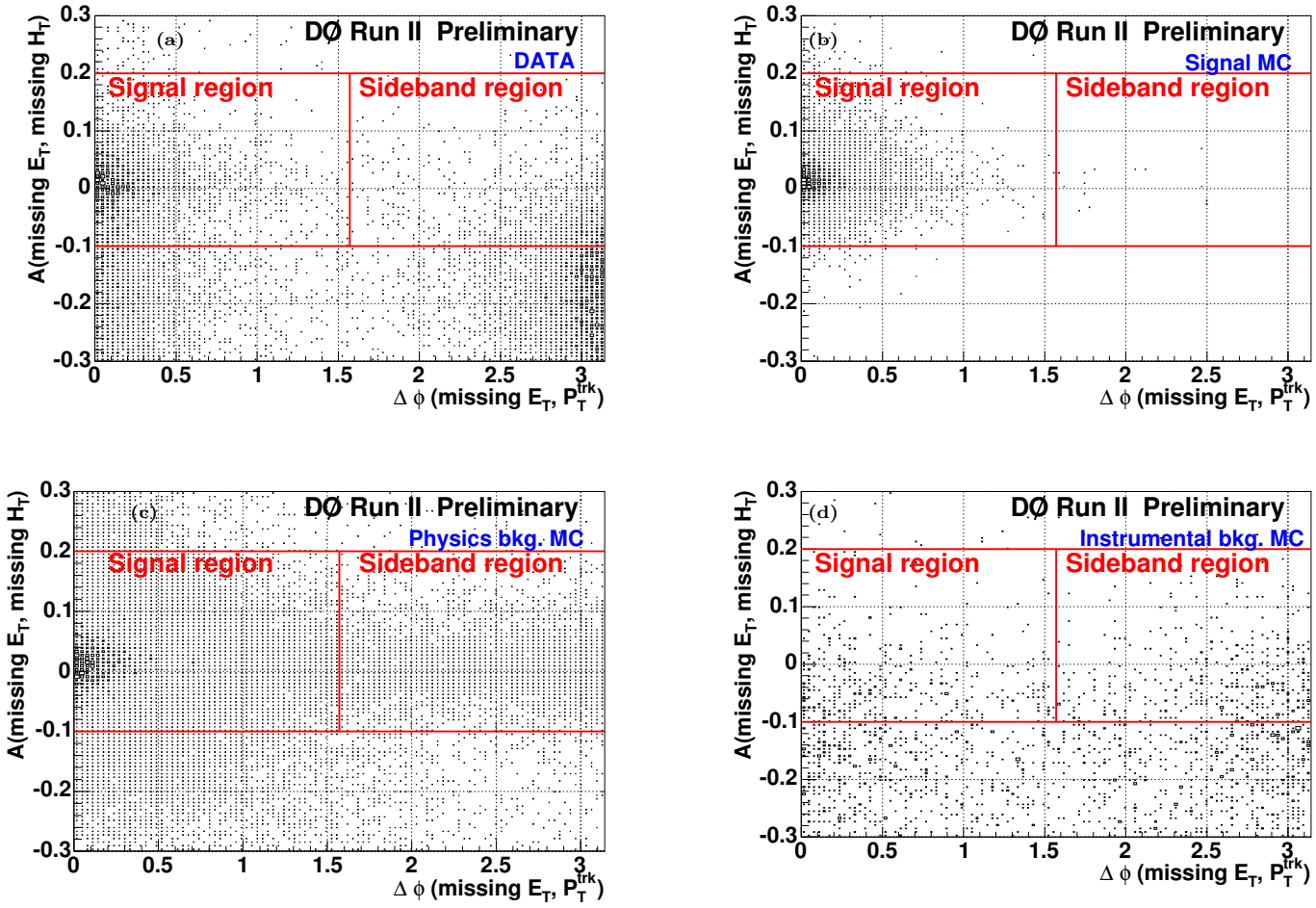

FIG. 2: Scatter plot of the A($\not\!\!E_T$, $\not\!\!H_T$) and $\Delta\phi(\not\!\!E_T, \vec{P}_T^{trk})$. (a) Data, (b) signal simulation, (c) physics background simulation, and (d) instrumental background simulation. The two boxes show the signal region and sideband region.

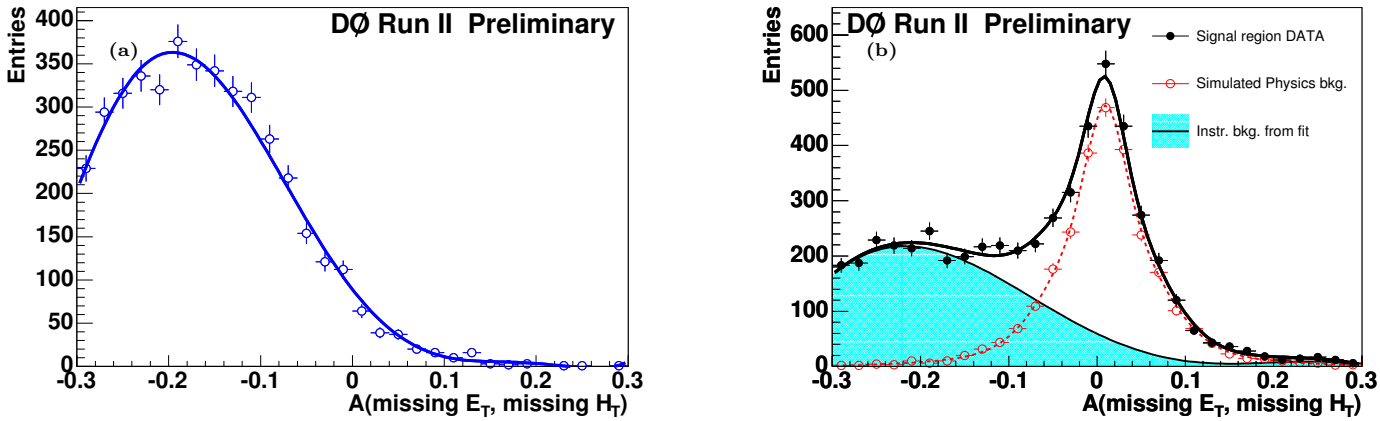

FIG. 3: A($\not\!\!E_T$, $\not\!\!H_T$) for (a) data in the sideband and (b) data in the signal region, physics background and instrumental background. A fit of a triple Gaussian + polynomial describe the data well. From the fit, 696.1 ± 91.4 instrumental bacground events are expected.

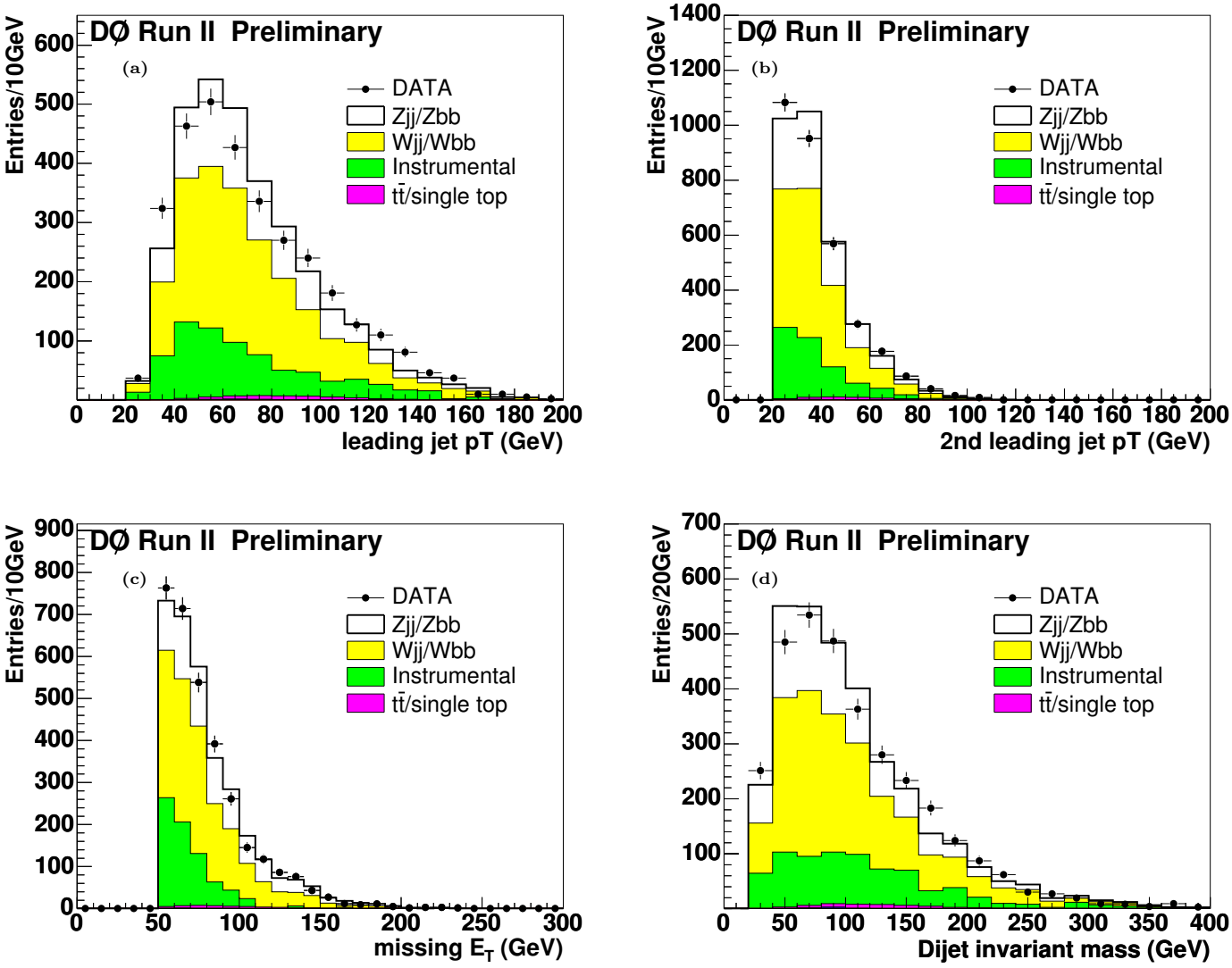

FIG. 4: The distributions after all selections except for b-tag. After acounting for instrumental background, the simulation agrees well with data. (a) p_T of the leading jet, (b) p_T of the second leading jet, (c) $\not\!\!E_T$, and (d) invariant mass of two leading jets.

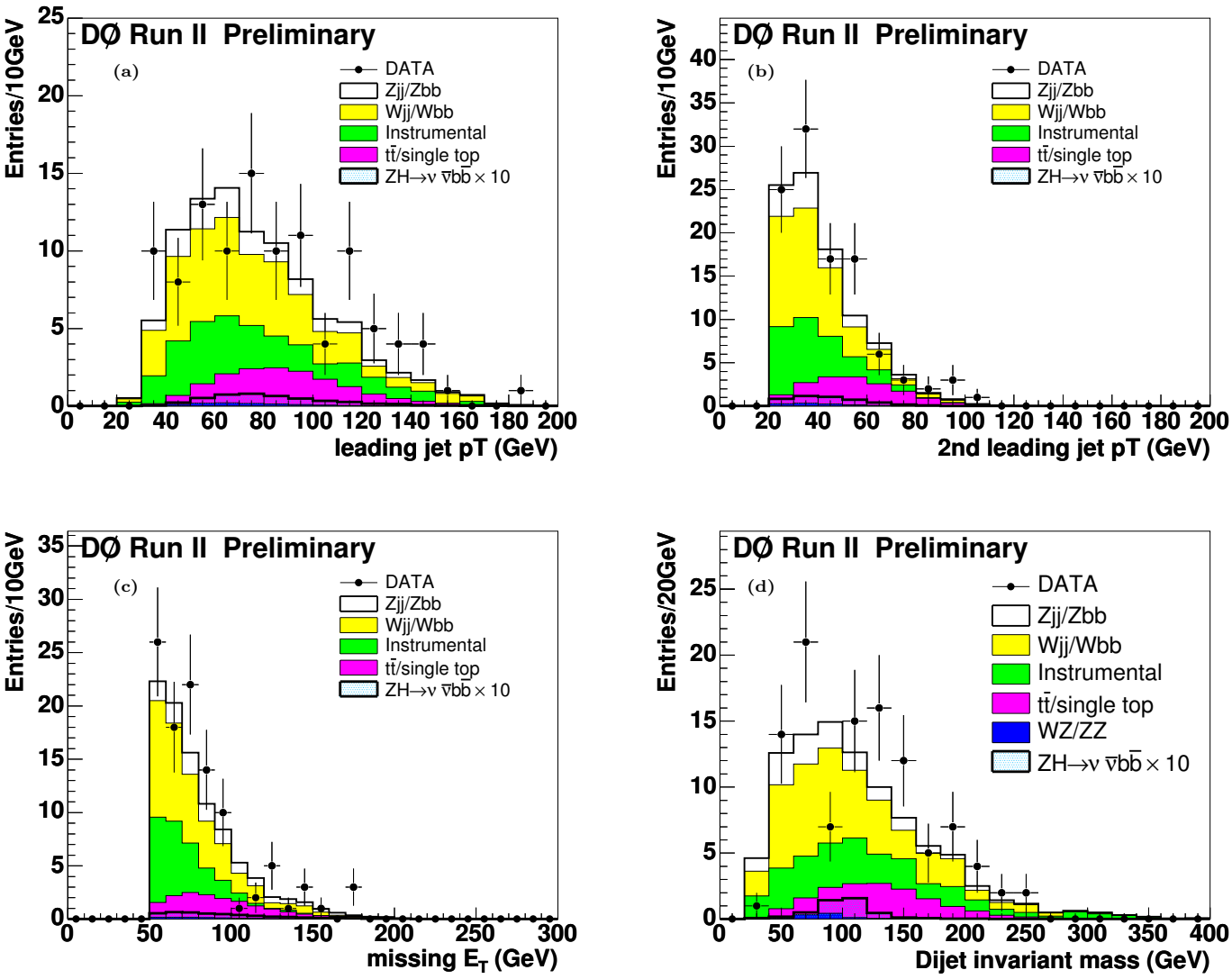

FIG. 5: The distributions in exclusive single b-tagged sample. (a) p_T of the leading jet, (b) p_T of the second leading jet, (c) $\not\!\!E_T$, and (d) invariant mass of the two leading jets.

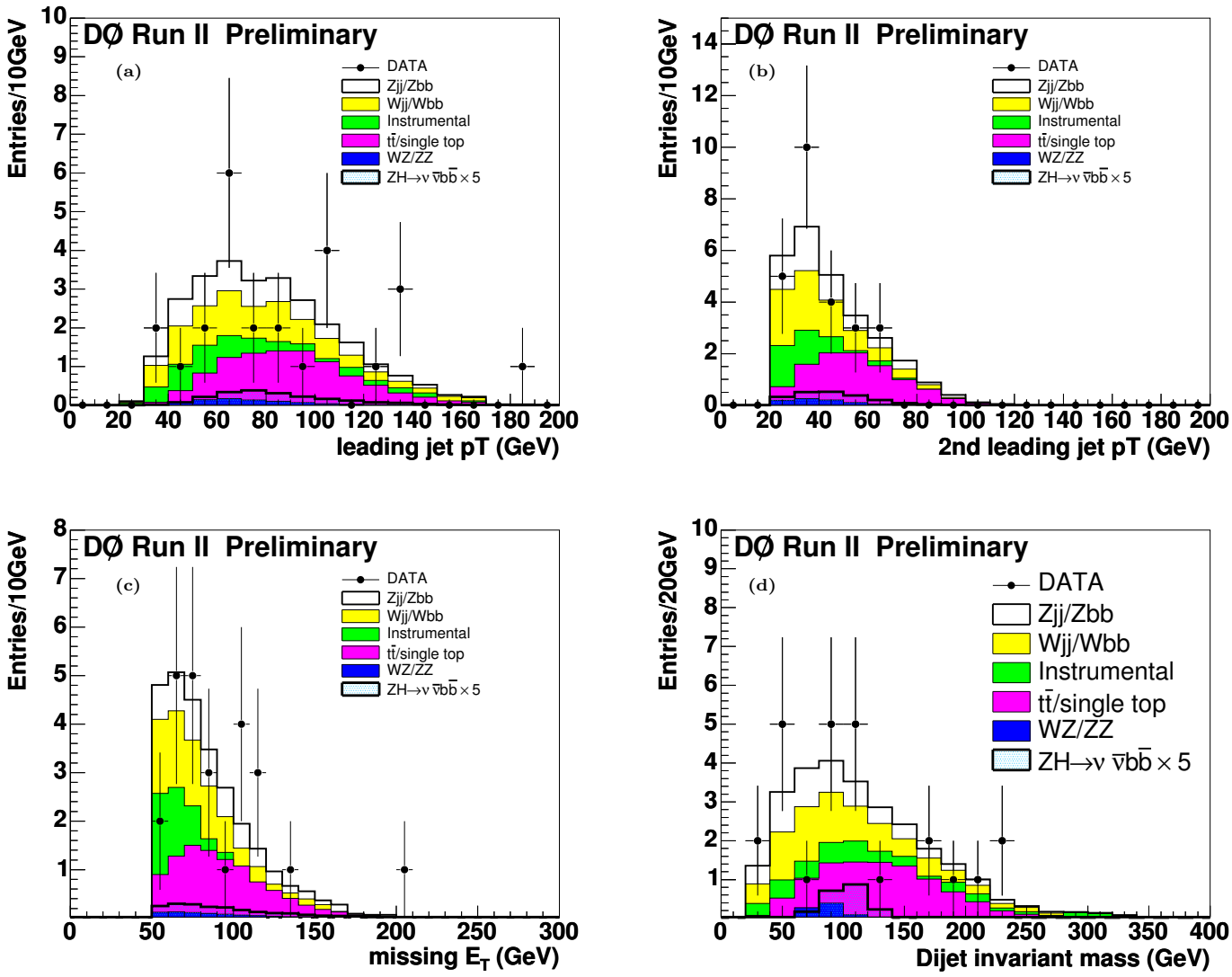

FIG. 6: The distributions in the double b-tagged sample. (a) p_T of the leading jet, (b) p_T of the second leading jet, (c) $\not\!\!E_T$, and (d) invariant mass of the two leading jets.

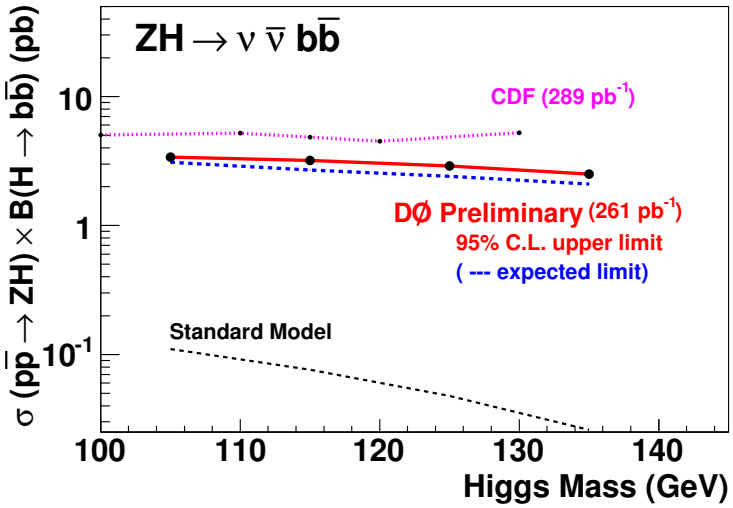

FIG. 7: 95% confidence level upper cross section limit (and corresponding expected limit), obtained by this analysis with 261 pb^{-1} of integrated luminosity, on ZH production versus Higgs mass. Also shown CDF preliminary analysis (289 pb^{-1}) [17] and the Standard Model expectation.